



Large-sized quasi-crystals with continuously adjustable compositions

Zijing Li ^{a, b}, Linran Zhao ^a, Shaopeng Pan ^c, Changzeng Fan ^a, Jianbing Qiang ^d,
Chuang Dong ^d, Li-Min Wang ^{a, *}

^a State Key Lab of Metastable Materials Science and Technology, College of Materials Science and Engineering, Yanshan University, Qinhuangdao, 066004, Hebei, China

^b Key Lab for Microstructural Material Physics of Hebei Province, School of Science, Yanshan University, Qinhuangdao, 066004, Hebei, China

^c College of Materials Science and Engineering, Taiyuan University of Technology, Taiyuan, 030024, Shanxi, China

^d Department of Materials Engineering, Dalian University of Technology, Dalian, 116024, Liaoning, China

ARTICLE INFO

Article history:

Received 8 November 2017

Received in revised form

26 February 2018

Accepted 27 February 2018

Available online 6 March 2018

Keywords:

Quasi-crystals

Intermetallic compounds

Solidification

Element addition

ABSTRACT

The quasi-crystal-forming alloys with adjustable compositions were prepared by element-addition to a pre-existing pure quasi-crystalline system. The protocol alloy $Zr_{40}Ti_{40}Ni_{20}$ was chosen as the parent alloy, and beryllium was used as the additive element. The quasi-crystal forming ability was found to be enhanced with Be content within a wide composition range of $(Zr_{40}Ti_{40}Ni_{20})_{100-x}Be_x$ ($0 \leq x \leq 16$). A maximum size of up to 10 mm in diameter of pure quasi-crystalline rod was attained at a composition of $(Zr_{40}Ti_{40}Ni_{20})_{84}Be_{16}$. Structural analyses show that Be-addition continuously reduces the interplanar spacing. The mechanism of the enhanced quasi-crystal forming ability was also discussed.

© 2018 Elsevier B.V. All rights reserved.

Since the discovery of the first quasi-crystal (QC) in Al–Mn alloy [1,2], the aperiodic solid with long-range order and rotational symmetries has attracted much research attention due to its unusual structure [2] and unique chemical and physical properties [3–8]. In this new research area, made possible by the discovery of QC, as continuous attempts have been made, hundreds of QCs have been found in different kinds of alloys [7,9–11]. Most QCs usually coexist with other crystalline phases, which is partly ascribed to the fact that the formation of pure QCs depends strongly on the alloy composition [12,13]. However, pure QC alloys are highly desirable for detailed studies of their structures, properties and potential practical applications [14–19]. Despite the considerable efforts made to date, only a limited number of pure QC-forming systems have been reported, especially in the case of bulk QC-formers of large size [12–14,20–28]. Thus, the search for new, pure QCs, and in particular, bulk pure QCs remains important.

It is argued that minor alloying is an effective method to stabilize QCs or enhance the fraction of QCs by modifying solidification processes or suppressing competitive crystalline phases [14,18,29–36]. Naturally, following this practice is the idea that new

pure QC alloys might be achieved by introducing specific elements to pre-existing pure QCs. However, such studies are rarely reported, which may be limited by the composition sensitivity of QC. In this work, the alloys of $(Zr_{40}Ti_{40}Ni_{20})_{100-x}Be_x$ were selected to test the feasibility of this idea. The parent alloy of $Zr_{40}Ti_{40}Ni_{20}$ has been tested as an optimal composition [9,13], with which a near-pure QC rod of 3 mm in diameter could be prepared. Beryllium was selected as the alloying element for two reasons: (1) its small atomic size, (2) the comparable interatomic interactions of Be with Zr and Ti to that of Ni with Zr and Ti as indicated by the mixing enthalpies (-43 kJ/mol for Be with Zr, -30 kJ/mol for Be with Ti, -49 kJ/mol for Ni with Zr, and -35 kJ/mol for Be with Ti) [37]. The experimental results show that the quasi-crystal forming ability (QCFA) of the alloys can be significantly improved by adding Be. A nearly pure QC rod of $(Zr_{40}Ti_{40}Ni_{20})_{84}Be_{16}$ of 10 mm diameter has been attained, which is significantly larger than that of $Zr_{40}Ti_{40}Ni_{20}$, giving a comparable result with the largest size recorded for a few QCs [28,32,38]. More interest is that nearly pure QCs of $(Zr_{40}Ti_{40}Ni_{20})_{100-x}Be_x$ can be achieved across a wide composition range ($0 \leq x \leq 16$), which is incompatible with the empirical knowledge that pure QCs usually form only at specific compositions.

Homogeneous ingots of $(Zr_{40}Ti_{40}Ni_{20})_{100-x}Be_x$ ($x = 0, 4, 8, 12, 16$, and 20 mol%) were prepared by melting the mixtures of high-purity metals five times in an arc-melting furnace. Then the

* Corresponding author.

E-mail address: liming_wang@ysu.edu.cn (L.-M. Wang).

alloys were cast into copper moulds of different diameters, by which the maximum diameters (d_{QC}) of QC rods were also determined. It should be noted that the values of d_{QC} might be subjected to some error (<2 mm) due to the discrete diameter of the copper moulds used. The structures of the plate samples cut from the as-cast rods were examined by X-ray diffraction (XRD) with Cu-K α radiation (Shimadzu XRD-6000 diffractometer) and transmission electron microscopy (TEM) using a JEOL-100FX microscope. The TEM specimens were prepared using standard twin-jet electrolytic thinning with HClO $_4$ -CH $_3$ OH mixture electrolyte (volume ratio 1:9). The thermal analyses of the samples were performed on a Perkin-Elmer Differential Scanning Calorimeter (DSC) 8000.

Fig. 1 shows the XRD patterns of the quenched samples of $Zr_{40}Ti_{40}Ni_{20}$, $(Zr_{40}Ti_{40}Ni_{20})_{92}Be_8$, $(Zr_{40}Ti_{40}Ni_{20})_{84}Be_{16}$, and $(Zr_{40}Ti_{40}Ni_{20})_{80}Be_{20}$ under two different cooling rates. The XRD results illustrate that the three former alloys can be quenched into near-pure QCs at relatively higher cooling rates. Further reductions in the cooling rate leads some other crystals to form which coexist with the QCs: these may be indexed as a C14 Laves phase and a β -Zr (Ti) solid solution [39]. By contrast, the amorphous signals appear in the as-cast rods of [15,20] mm diameter of $(Zr_{40}Ti_{40}Ni_{20})_{80}Be_{20}$, indicating that a lower cooling rate should be adopted for preparing pure QC rods (this remains beyond the limit of our current experimental conditions). Therefore, further studies were only carried out on the alloys of $(Zr_{40}Ti_{40}Ni_{20})_{100-x}Be_x$ ($0 \leq x \leq 16$). As shown in

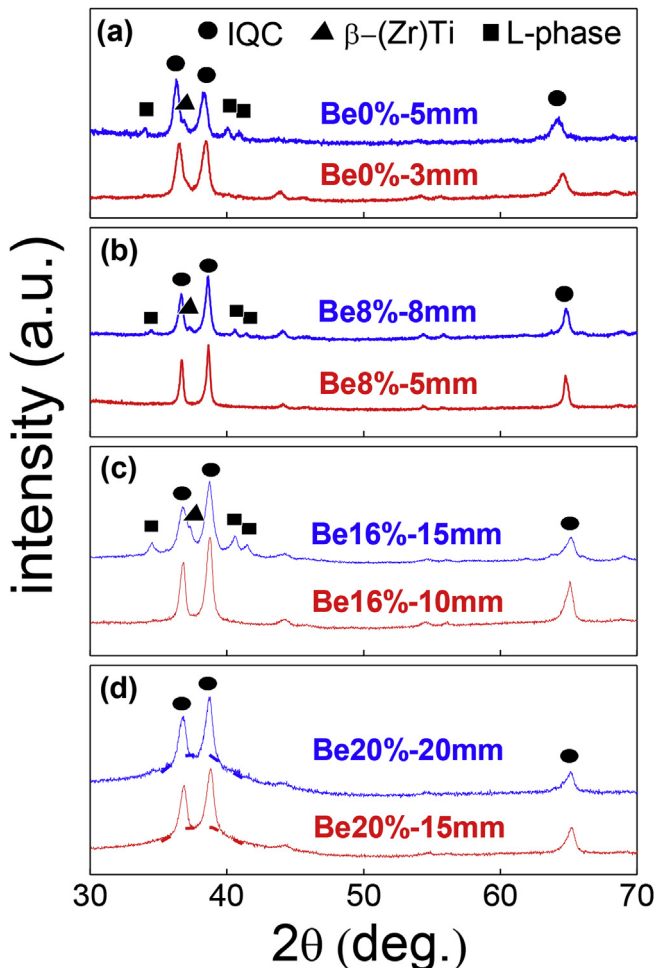


Fig. 1. XRD patterns of the suck-casted samples of (a) $Zr_{40}Ti_{40}Ni_{20}$, (b) $(Zr_{40}Ti_{40}Ni_{20})_{92}Be_8$, (c) $(Zr_{40}Ti_{40}Ni_{20})_{84}Be_{16}$, and (d) $(Zr_{40}Ti_{40}Ni_{20})_{80}Be_{20}$ of different sizes.

Fig. 1 (a) to (c), the phase sequence during solidification is from QC to the mixture of QC and stable crystals with decreased cooling rate, which is consistent with theoretical studies [40,41].

Fig. 2 (a) shows the XRD patterns of the QC rods of $(Zr_{40}Ti_{40}Ni_{20})_{100-x}Be_x$ obtained at the appropriate cooling rates. Except for the three main diffraction peaks (indexed in terms of Cahn's scheme) belonging to the QCs [42], no other crystalline signals could be detected in the XRD patterns, indicating their nearly pure QC nature. The enlarged XRD patterns in angle range from 36° to 40° are shown in the inset, where a continuous movement of the diffraction peaks is seen towards the high angle side with the increased Be content. According to Bragg's law, the interplanar spacings corresponding to the 18/29 diffraction peaks were determined and shown in Fig. 2 (b), indicating that Be-addition results in a monotonically reduced interplanar spacing. Additionally, Fig. 2 (b) also shows the Be-content dependence of the full width at half maximum (FWHM) of the 18/29 XRD peaks. With more Be atoms introduced into the parent alloys, the XRD peaks of the QC alloys become broader.

Fig. 3 demonstrates the TEM results of the as-cast rods of $(Zr_{40}Ti_{40}Ni_{20})_{92}Be_8$ and $(Zr_{40}Ti_{40}Ni_{20})_{84}Be_{16}$ with diameters of 3 and 10 mm, respectively. The bright field TEM images reveal that both of the samples consist of a primary crystalline phase and a small volume fraction of a glue-like phase between the crystal grains of the primary phase. The 2-fold, 3-fold, and 5-fold selected area electron diffraction (SAED) patterns obtained from the primary phase share the typical features of icosahedral QCs [1], while the amorphous nature of the glue-like phase could be identified by its halo diffraction pattern. Therefore, the samples were identified as being composed of the QC and amorphous phases, marked by Q and A, respectively. The QC phase is dominant in the two as-cast rods. The TEM image indicates the volume fraction of QC in the sample of $(Zr_{40}Ti_{40}Ni_{20})_{84}Be_{16}$ exceeds 95%. The relatively lower QC volume fraction in the 3-mm rod of $(Zr_{40}Ti_{40}Ni_{20})_{92}Be_8$ may be attributed to the higher cooling rate adopted for the sample than that in the case of $(Zr_{40}Ti_{40}Ni_{20})_{84}Be_{16}$. Taking into account the QC-forming composition of $Zr_{40}Ti_{40}Ni_{20}$ [13], we naturally came to the conclusion that, at the appropriate cooling rate(s), the alloys of $(Zr_{40}Ti_{40}Ni_{20})_{100-x}Be_x$ can be quenched into near-pure QCs across a wide composition range ($0 \leq x \leq 16$). This reveals an unusual behaviour of the QC alloys of $(Zr_{40}Ti_{40}Ni_{20})_{100-x}Be_x$ in that they are composition-adjustable, which remarkably contrasts with conventional QCs for which specific compositions are required [13,22,43].

To clarify the stability of the QC and the amorphous phases in the samples, thermal analyses of the as-cast and the annealed alloy rods of $(Zr_{40}Ti_{40}Ni_{20})_{84}Be_{16}$ of 8 mm in diameter were carried out. As shown by the red DSC curve in Fig. 4 (a), the as-cast sample undergoes two exothermic processes when being heated from 543 to 843 K. The exothermic heating occurred around the lower temperature of $T_{p1} = 733$ K and was only 0.458 kJ/mol, which was much less than that of the usual crystallisation process. The other exothermic process occurred at $T_{x2} = 831$ K. For comparison, the green curve shows the DSC result of the annealed sample at 803 K, where the weak exothermic peak at around 733 K disappeared, while no change was observed during the high temperature exothermic process. Fig. 4 (b) demonstrates the XRD patterns of the as-cast and the annealed samples of $(Zr_{40}Ti_{40}Ni_{20})_{84}Be_{16}$. Upon close observation of the XRD results, the sharp diffraction peaks were superimposed on the quite weak halo diffraction patterns. This indicates that the samples were composed of a dominant fraction of QC and a small amount of the amorphous phase, which matched the TEM results in Fig. 3. Compared to the as-cast sample, the intensity of the halo diffraction peak of the annealed sample decreased significantly, and except for the QC XRD peaks, no other

Download English Version:

<https://daneshyari.com/en/article/7992673>

Download Persian Version:

<https://daneshyari.com/article/7992673>

[Daneshyari.com](https://daneshyari.com)